Design of and Practical Experience with a Thermographic Crack Checking System using Laser Heating

Gerhard TRAXLER [1], Petra THANNER [1], Pauline MEYER-HEYE [1]

[1] PROFACTOR GmbH, Machine Vision, Office Vienna
Phone: +43 7252 885-951, Fax: +43 7252 885-951; e-mail: gerhard.traxler@profactor.at,
petra.thanner@profactor.at, pauline.meyer-heye@profactor.at

Abstract
A growing number of thermographic testing systems with laser heating are used, to ensure high quality of automotive components. They are installed in production lines for real time automatic crack checking.
When designing such a system many technical aspects as well as external limitations have to be considered, many of them are interdependent and some are even conflicting. A limiting external factor is the real time requirement. This means that the heat flow process has to be optimized to allow a quick checking procedure. On the other hand, the process must stay within the temperature range which the tested material can tolerate without damage. The main system components are laser, camera, piece handling and the computer controlling the hardware and running the testing software. Main objective of the components layout is to produce a thermal image that can be evaluated.
In this paper we describe the usage of a finite difference simulation to design the system including the right parameters with respect to their interdependences and the image processing. Further, the image processing is described as well as experience with the crack checking system and its limitations.

Keywords: thermography, laser beam profile, excess temperature, flying spot, non destructive evaluation (NDE), finite difference method (FDM), crack checking

1. Introduction

This paper describes a crack checking system with its design considerations for use in production lines, which means that it has to fulfil some basic conditions. One of these is the maximum checking time like stated for heavy samples [1], which must not exceed 2.5s, and the other one is the maximum excess temperature of 100°C to avoid damaging of the testing samples.

Main objective is to compensate the influence of the local distortions. From practical tests for laser induced crack checking on steel samples in the project ThermoBot[1][2], thermograms were found to be disturbed by local signal fluctuations of high amplitude, especially at locations close to laser excitement. Since this effect makes it harder to identify cracks, an alternative solution is searched, in which distortions are suppressed implicitly. First step, described in this paper is to investigate a solution for circular and well known path, even if the laser spot will randomly move along a path, controlled by a robot in the later application. Adaption to a randomly moving laser situation is then planned to be done by tracking of the samples surface in a small patch, given by the known path. To avoid confusion and to focus onto distortion-compensation we use an application example with circular laser spot, in which the path of the laser-spot as well as the movement of the surface is well known.

Design of the automated checking system started with a general idea of the testing process and a basic experiment. In detailed planning a simulation was used to define and evaluate all

[1] 7th framework project, see Acknoledgements

main system parameters. This step by step procedure has been done, to avoid risks in later stages of the project.

The idea for the checking method was to put the testing sample onto a turntable, and to heat up single spots by a laser. A thermal camera takes image sequences from the area around the hot spot to generate data for evaluation.

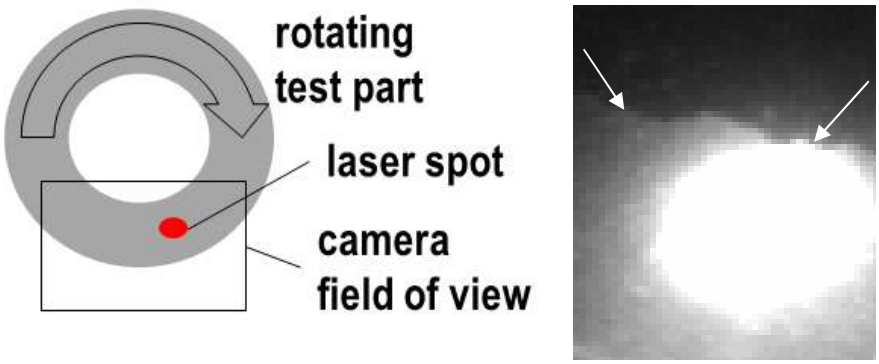

Figure 1. Image position and sample thermogram of a crack

First data about feasibility and material properties were then generated in a first test, in which the testing sample didn't move. As displayed in figure 1 the crack, marked by arrows in the thermal image can be recognized.

In addition, the material parameters, density $\rho = 7030\mathrm{kgm}^{-3}$, specific heat capacity $c_p = 413\mathrm{Jkg}^{-1}\mathrm{K}^{-1}$, thermal conductivity $\lambda = 73\mathrm{Wm}^{-1}\mathrm{K}^{-1}$ and thermal diffusivity $\kappa = \frac{\lambda}{\rho c_p} = 45\mathrm{m}^2\mathrm{s}^{-1}$ were investigated as they are needed for the design. Another parameter, namely the effect caused by local emissivity was found to be smaller or equal to 1K.

2. Design

As usual in design upfront calculations were necessary, since not all the eligible hardware components could be tested out in the first experiment. As the test result quality depends on all the hardware components as well as the image evaluation method, a mathematical representation of the whole system was needed. A simulation based on the finite difference method (FDM), like used to find crack sensitivity [3] was implemented to describe the parameters of the crack checking system (1).

$$\Delta T^{t+\Delta t}_{x_2y_2z_2} = \Delta T^{t+\Delta t}_{x_2\leftarrow x_3} + \Delta T^{t+\Delta t}_{x_2\leftarrow x_1} + \Delta T^{t+\Delta t}_{y_2\leftarrow y_3} + \Delta T^{t+\Delta t}_{y_2\leftarrow y_1} + \Delta T^{t+\Delta t}_{z_2\leftarrow z_3} + \Delta T^{t+\Delta t}_{z_2\leftarrow z_1} =$$

$$= \frac{\kappa\Delta t}{\Delta x\Delta y\Delta z}\left(\begin{array}{l} \frac{T_{3,2,2} + T_{1,2,2} - 2T_{2,2,2}}{\Delta x}\Delta y\Delta z + \\ + \frac{T_{3,2,2} + T_{1,2,2} - 2T_{2,2,2}}{\Delta y}\Delta x\Delta z + \\ + \frac{T_{2,2,3} + T_{2,2,1} - 2T_{2,2,2}}{\Delta z}\Delta x\Delta y \end{array}\right) = \quad (1)$$

A 3-dimensional model of the test object, a highly thermally conducting ring, with 20mm outer diameter and a height of 5mm has been constructed by use of 100 x 100 x 25 cubes, each of 200µm length. Cracks were inserted by setting the local heat transfer coefficient to 90 $Wm^{-2}K^{-1}$ at locations displayed in figure 2. All surfaces of the model at a starting temperature of 25°C transfer energy into surrounding air of 25°C, defined by a heat transfer coefficient of 45 $Wm^{-2}K^{-1}$.

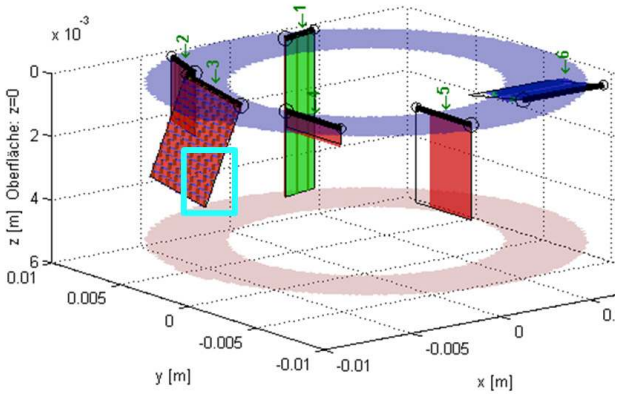

Figure 2 Cracks in the FDM-Model

Energy transfer from the laser to the surface elements of the model was taken into account by a two-dimensional Gaussian-distribution of local laser power. For each temporal step in the simulation laser energy was simply added to surface elements, depending on their location in relation to the laser beam.

3. Evaluation

Subsequent evaluation of the image sequence is designed to enhance contrast and to assemble one image as intermediate result from the series of images. As displayed in figure 1, only a part of the surface area is captured by the camera. For assembly of the thermal sequence into one intermediate result image of the entire sample, each of the single images has to be transformed from camera-coordinates into testing sample coordinates. The resulting image should display a high contrast of temperature steps, which are assumed to be caused by cracks.

Beside of standard pre-processing in thermographic applications like non uniformity correction and bad pixel replacement [4] the area, directly covered by the laser spot is reset to some base value. This is necessary due to the extreme high amplitude in the laser spot center and the high gradient near to it. Since we want to produce images of high contrast at steps, a gradient image will be calculated by computation of the partial values in x and y-direction first, and the absolute value next (2).

$$
\begin{aligned}
g_{x(x,y)} &= T_{(x+1,y)} - T_{(x,y)} \\
g_{y(x,y)} &= T_{(x,y+1)} - T_{(x,y)} \\
g_{(x,y)} &= \sqrt{g^2_{x(x,y)} + g^2_{y(x,y)}}
\end{aligned}
\tag{2}
$$

Once the entire thermal sequence is converted into gradient images, coordinate transformation and accumulation is done like shown in figure 3. Based on the image coordinates of the rotational axis, the area of interest in the gradient image is rotated and shifted to fit into coordinate system of the result image, having its origin in the center. No scaling is necessary, since both systems are measured in pixel. If the thermal sequence contains all images, captured in the time frame of one revolution of the testing sample, we get an image of the entire sample in the result image.

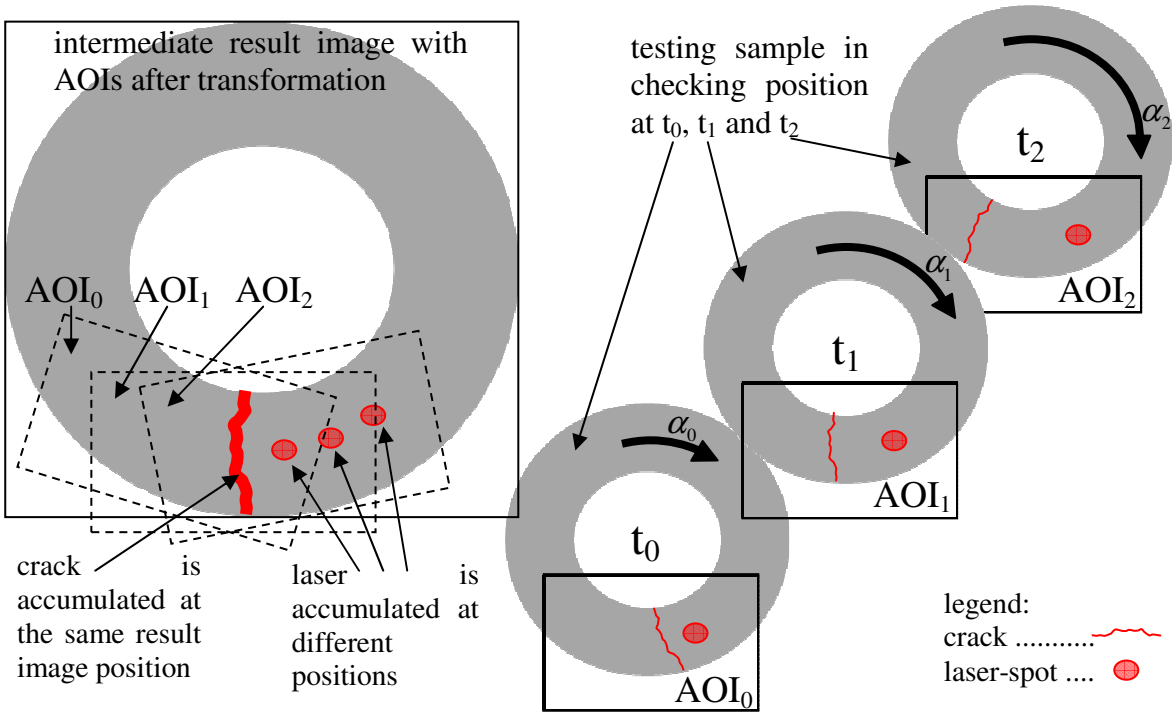

Figure 3. Principle of coordinate system transformation with suppression of laser-spot

In the consecutive images a crack is stationary, while the laser spot is moving. A crack will be added to the result about 20 to 50 times at the same coordinates, while a laser spot is added only one time at every coordinate of its movement, and thus is suppressed in relation to the crack signal.

To avoid getting edges of the testing sample as crack results, masking out of locations close to edges must be done with the intermediate result, which is input for the next evaluation steps to identify crack locations. Due to smallest quantisation size being one pixel, we call a location, which is assumed to be part of a crack a crack-pixel. Starting with segmentation for just the strongest signal amplitudes in the intermediate result image, crack-pixel found get the function of a seed. In an iterative process crack-pixels with stepwise decreasing signal amplitude are searched, and checked, if they are neighbours to already existing seeds, resulting in crack segments of successive growing length. In addition directional relation is

checked in the way to add maximum one new crack-pixel at each segment end, resulting in a line of one pixel width, but not in a crack-pixel area at all. Distance and orientation of the segment ends are connected to each other, if they are close neighbours in the next evaluation step. A crack is then defined by a crack segment longer than a pre-adjusted minimum length, which typically is in the range of some pixel.

4. Results

4.1 Design

After optimization of checking duration by variation of parameters and repeated simulations a laser power of 12W with a Gaussian beam profile ($\sigma = 0.3\text{mm}$), moving with 0.5 rpm has been found to fit to the requirements. This heat source induces crack-signal amplitude high enough to be detected by a thermal camera at a frame rate of 250Hz. In each simulation-run the overall energy balance (3) was checked to assure a small error in the calculations.

$$Q_{Error} = Q_{End} - Q_{Start} - Q_{Absorbed} + Q_{Env} \tag{3}$$

With a duration of 2s, the absorbed energy is $Q_{Absorbed}$=24J and the energy transferred into environment is Q_{Env}=0.58J. Q_{Start} and Q_{End} are the sum of energy of all elements in the model before start of simulation and after its end. A typical error Q_{Error} was less than 1nJ, which is at least 10 orders below of laser energy, and in turn negligible for further interpretation of the surface temperature distributions.

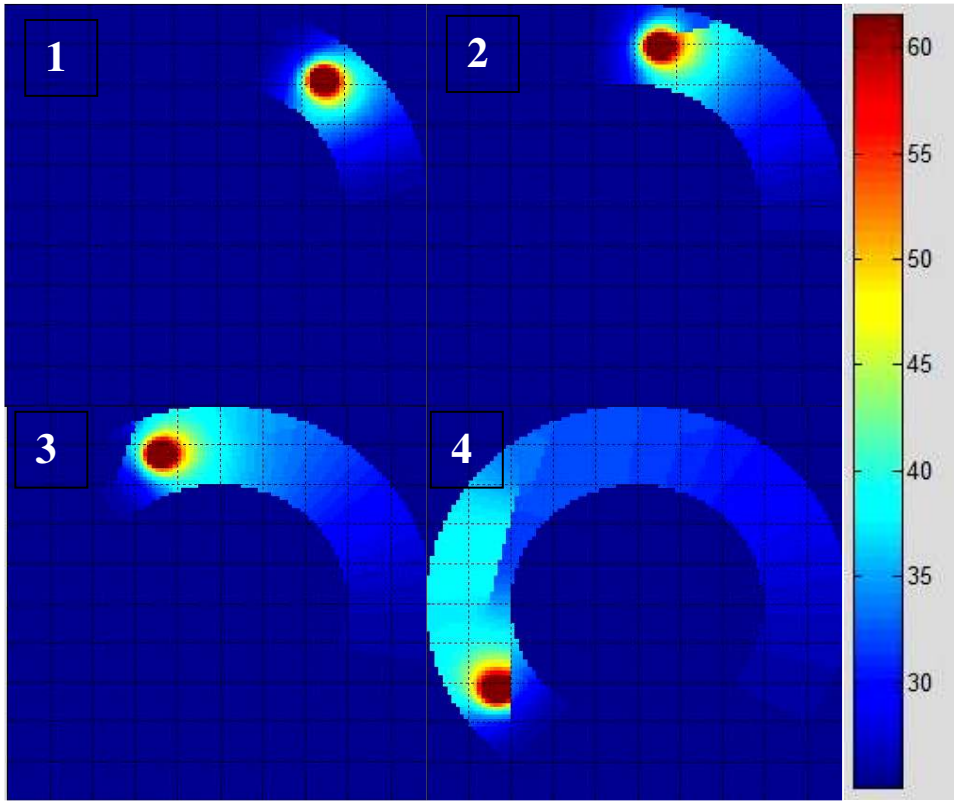

Figure 4: Temperature distribution [°C] for different laser spot locations; 1: no crack, 2: laser spot passes crack, 3: laser spot approaches crack 4: laser spot close to crack of small depth

Image 1 in figure 4 displays the surface temperature distribution if there is no crack in the testing object. Any temperature profile along of a line inside the surface is continuous, and stepless respectively. A step of up to 15K occurs at the edges of the model. In image 2 and 3 a temperature step of aproximately 10K appears inside the surface area at the crack location. Some of the cracks in image 4, which has been passed by the laserspot still shows smaller temperature steps, while the temperature step at the crack close to the spot allready starts to diminish. This effect is expected due to the smaller depth of the crack, which is close to the laser spot in image 4.

Practical experience with the crack checking system confirmed the design to a large extent. Depending on the surface quality of the test items, the laser power was adjusted to 15W – 20W, which is a little less than designed (24W). A typical crack-signal has an amplitude approximately 10 times above noise equivalent temperature difference (NEDT) of the camera, so even weak cracks are visible.

4.2 Evaluation

Unfortunately some artefacts, caused by locally high temperature gradients are also contained in the gradient images. Figure 5 shows two example gradient-images, containing the outline of the outer diameter, a crack and an artefact from the locally high temperature gradient close to the laser in the right image (marked by a dotted circle).

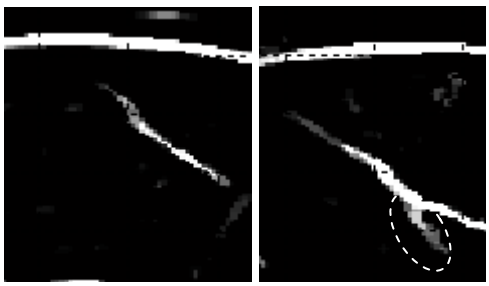

Figure 5. typical AOI with crack (left image) and crack and artefact (right image)

The artefacts could be masked out by enlargement of the laser-mask at the cost of sensitivity and the extent of the evaluated area, which both is not preffered. Therefore, as described in chapter "3. Evaluation" the gradient images are transformed into intermediate result images, and simply accumulated there. As expected, the artefacts are ocurring only once, while crack segments ocurrs 20 times typically. In turn, the crack signals are amplified approximatly one order more than the artefact signals, when assembled into the intermediate result image in figure 6.

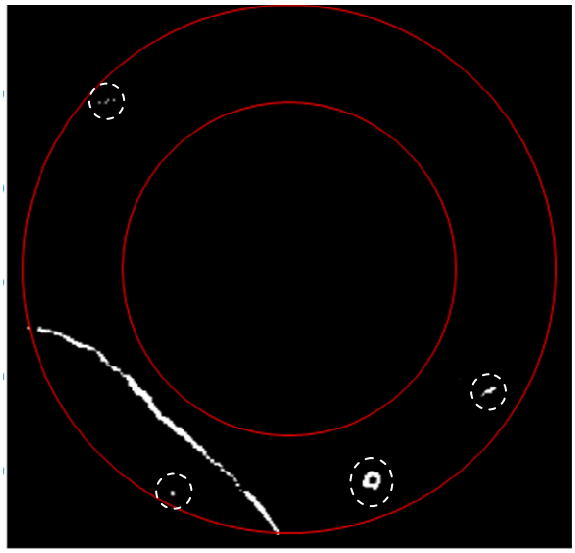

Figure 6. intermediate result image (250 x 250 pixel), constructed by accumulation of gradient images

Figure 6 shows an example of an intermediate result image, in which the outlines, marked by solid circles in the image were already masked out. Beside of the crack some remaining small artefacts are displayed, marked by dotted circles. They were caused by local reflection (dots, line) and by an impurity (circle). Based on their small size and their geometry they are not classified as crack.

Cracks located very close to the items edge are problematic to be classified correctly. This is not caused by heat flux method, since the crack signal will be generated, but more a problem of spatial aspects. The edge of the item looks like a strong crack, because the flux of heat is disrupted here. In consequence there are two crack-like signals, which are located very close to each other. Each crack consists of a number of single defect pixels that are aligned to form a crack. All pixels that are below the threshold for the minimum gap between two cracks are merged. This method can misinterpret two cracks that are orientated in parallel and located close to each other as only one crack, e.g. two short cracks in the material resulting in one result crack. This is unproblematic unless a crack is close to the test specimen's edge. The crack pixels are in such case merged with the crack-like pixels that represent the edge. The crack location is tested against the geometry data and the crack might be ruled not to be a crack but the material border and is thus not present in the results. The ability of the testing system to correctly distinguish the crack from the edge depends mainly on limited geometry mapping accuracy, which typically was in the range of +/-1pixel. Due to stability aspects, the mask for skipping edge-signals was set to be +/-2 pixels. In consequence cracks closer than 2 pixels to the edge couldn't be identified.

5. Conclusions

We have shown that design parameters for laser induced crack checking found by FDM-simulation fit quite well to practical parameters, and therefore FDM can be used for dimensioning of laser power, spot geometry, spot velocity and frame rate. Practical tests confirmed our expectations about amplification of crack signals one order above amplification of laser artefact signals. In consequence the proposed method of multiple accumulations of

gradient images has proven to be effective for improvement of thermal signal. We achieved better separation between crack- and artefact-signals and reduced errors in crack classification in turn.
The problem of masking out cracks close to the edges of the testing sample couldn't be solved. It is marking the limitation for the surface area, in which successful crack checking is possible.

6. Outlook

Since the application example restricted itself to a simple and well known path of the laser spot, further work is planned to make the proposed method usable with random paths too. In a composition with a testing sample, moved by a robot, path data are transferred to the crack-evaluation unit. Since path data are of limited accuracy, tracking of surface location is planned to be used for fine adjustment of the laser spot path.

Acknoledgements

This work was supported by the European Commission in the 7th Framework program under grant No. 284607, project ThermoBot.

References

[1] J. Schlichting, M. Ziegler, C. Maierhofer, M. Kreuzbruck, Flying Laser Spot Thermography for the Fast Detection of Surface Breaking Cracks, Proceedings 18th World Conference on Non-Destructive Testing, Apr. 2012. [Online]. Available: http://www.ndt.net/article/wcndt2012

[2] ThermoBot, Autonomous robotic system for thermo-graphic detection of cracks, 2012-2014, http://thermobot.eu/

[3] Li, T., Almond, D. P. and Rees, D. A. S. , 2011. Crack imaging by scanning laser-line thermography and laser-spot thermography. Measurement Science & Technology, 22 (3), 035701.

[4] M. Vollmer, K.-P. Möllmann, Infrared Thermal Imaging: Fundamentals, Research and Applications, ISBN 978-3-527-40717, 2010 Wiley-VCH Verlag GmbH & Co.KGaA, Boschstr. 12. 69469 Weinheim, Germany